Ultracompact binary pulsars as continuous dual-line gravitational-wave Sources

Wen-Cong Chen (陈文聪)
Qingdao University of Technology
(青岛理工大学)

Jinan, FPS10, Jul 15

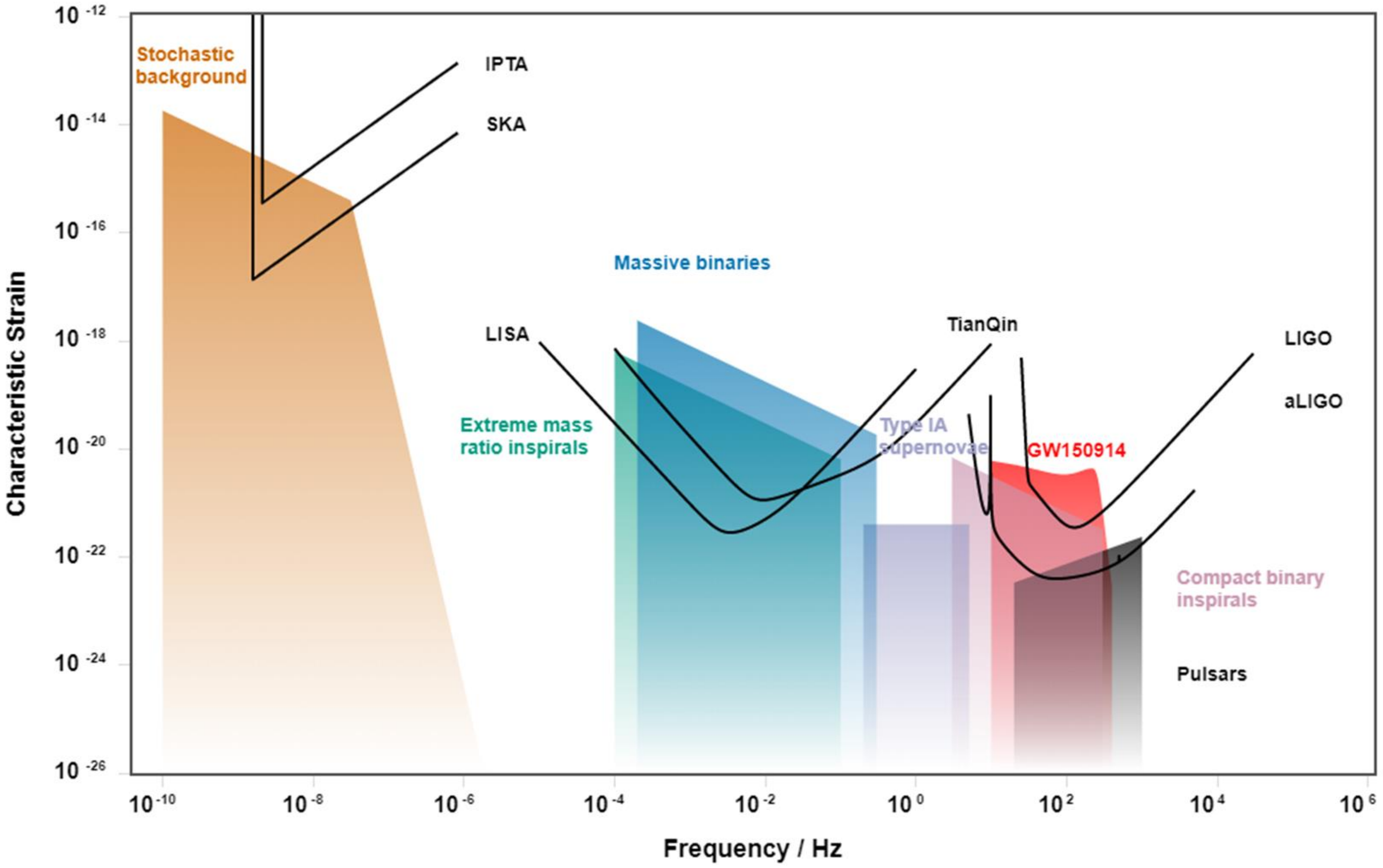

Characteristic Strain
Frequency / Hz
10^{-12}
10^{-14}
10^{-16}
10^{-18}
10^{-20}
10^{-22}
10^{-24}
10^{-26}
10^{-10}
10^{-8}
10^{-6}
10^{-4}
10^{-2}
10^{0}
10^{2}
10^{4}
10^{6}
Stochastic background
IPTA
SKA
Massive binaries
LISA
TianQin
LIGO
aLIGO
Extreme mass ratio inspirals
Type IA supernovae
GW150914
Compact binary inspirals
Pulsars

Detectability of GW candidate sources

- Ultra-compact X-ray binaries (UCXBs)
  neutron star (NS) + main sequence (MS) (Chen et al. 2020, ApJL)
  NS+ He star (Wang et al. 2021, MNRAS, in press)

- AM CVn star
  white dwarf (WD) + MS (Liu Jiang & Chen 2021, ApJ)
  WD+ He star (Liu et al. 2021, in preparation)

- Intermediate-mass black hole X-ray binaries (Chen 2020, ApJ, Han Jiang & Chen 2021, ApJ)
- Binary millisecond pulsars (Chen 2020, PRD; Chen 2021, PRD)

Binary pulsar-LISA source

NS+MS channel:

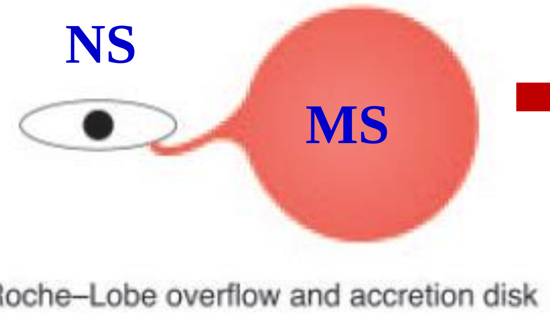

LMXB/IMXB

NS+He core
Detached system
with ~0.3 days

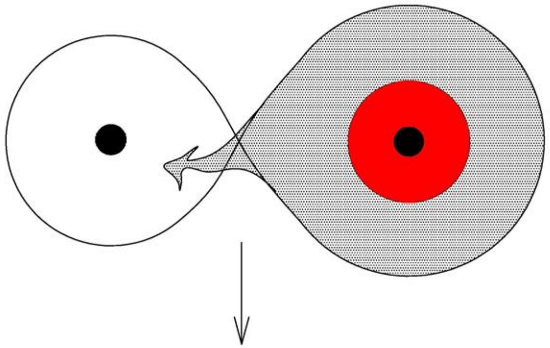

UCXB

orbital period < 1.0-1.5 hours

MESA

Table 1

Selected Evolutionary Properties for UCXBs and Their Progenitors for Different Initial Donor Star Masses and Initial Orbital Periods

$M_{\rm d,i}$ ($M_\odot$)	$P_{\rm i,orb}$ (days)	$t_{\rm rlov}$ (Gyr)	$t_{\rm deta}$ (Gyr)	$P_{\rm deta}$ (days)	$M_{\rm wd}$ ($M_\odot$)	$t_{\rm ucxb}$ (Gyr)	$P_{\rm ucxb}$ (days)	$P_{\rm min}$ (minutes)	$f_{\rm i,LISA}$ (mHz)	$\Delta t_{\rm LISA}$ (Myr)
2.0	2.89	0.83	3.45	0.297	0.170	9.16	0.004	4.94	0.83	34.9
2.5	2.79	0.44	2.89	0.319	0.166	9.49	0.004	5.12	0.84	34.8
3.0	2.72	0.26	2.69	0.274	0.160	6.02	0.005	5.83	0.87	14.0
3.3	2.70	0.20	2.43	0.347	0.165	10.86	0.004	5.14	0.87	34.6

Note. The columns (from left to right): the initial donor-star mass, the initial orbital period, the stellar age at the beginning of Roche lobe overflow, the stellar age, and the orbital period when the binary becomes a detached system; the WD mass, the stellar age, and the orbital period when the system appears as a UCXB; the minimum orbital period; the initial GW frequency that the binary is detectable by LISA; and the timescale that the binary appears as LISA source.

Chen et al. 2020, ApJL

The detections of low-frequency GW signals can accurately constrain the masses of NSs (Tauris 2018, PRL)

$$\mathcal{M} = \frac{c^3}{G}\left(\frac{5\pi^{-8/3}}{96} f_{\rm gw}^{-11/3}\dot{f}_{\rm gw}\right)^{3/5},$$

$$\mathcal{M} = \frac{(M_{\rm ns}M_{\rm d})^{3/5}}{(M_{\rm ns}+M_{\rm d})^{1/5}}.$$

Dual-line detection in low-frequency and high-frequency GW bands?

Continuous high-frequency GW radiating by rotating NSs

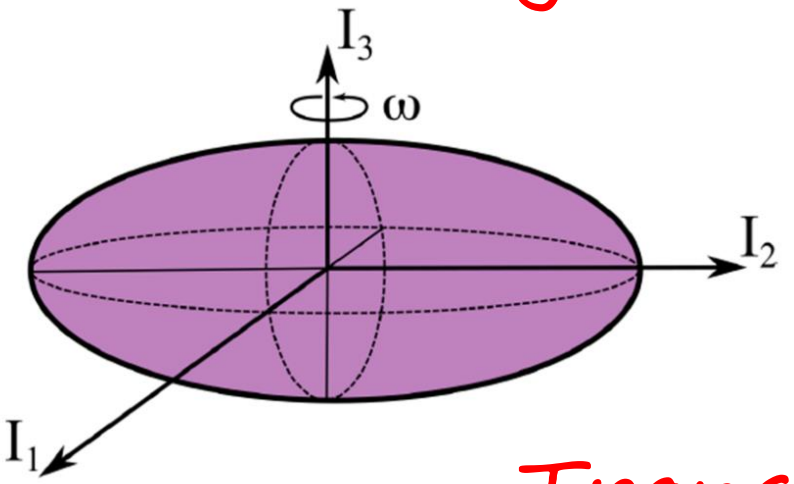

Ellipticity:

$$\epsilon = (I_1 - I_2)/I_3$$

Transitional MSPs

TABLE II. Some derived parameters for three transitional MSPs.

Sources	$\dot{M}_{acc}$ (10^{13} g s^{-1})	$\dot{M}_{13}$	r_m (10^6 cm)	r_{co} (10^6 cm)	r_{lc} (10^6 cm)	$\dot{\nu}_{ac}$ (10^{-16} Hz s^{-1})	$\dot{\nu}_{pr}$ (10^{-15} Hz s^{-1})	$\dot{\nu}_{gr}$ (10^{-15} Hz s^{-1})	ϵ (10^{-9})	η (10^{-31} s)
J1023	1.62	10	5.7	2.4	8.1	0.83	−1.6	−1.52	0.9	1.2
J12270	2.27	14	5.2	2.4	8.1	1.1	−1.85	−2.16	1.0	1.4
J18245	540	540	1.8	4.2	18.9	158	0	−15.79	23.4	15.3

(Chen 2020, PRD)

Redbacks

TABLE III. Constraints on the ellipticity of twelve redbacks with observed spin-down rates.

Sources	ν (Hz)	$\dot{\nu}$ (10^{-15} Hz s^{-1})	d (kpc)	$\dot{\nu}_{\rm md}$ (10^{-16} Hz s^{-1})	$\dot{\nu}_{\rm gr}$ (10^{-15} Hz s^{-1})	ϵ_{-9}	h_c (10^{-27})
PSR J1048 + 2339	214.35	−1.38	2.0	−0.96	−1.28	10.25	1.0
PSR J1227-4853	592.99	−3.9	1.61	−20.23	−1.88	0.97	0.9
PSR J1431-4715	497.03	−3.486	1.56	−11.91	−2.29	1.67	1.1
PSR J1622-0315	260.05	−0.784	1.14	−1.71	−0.61	4.37	1.1
PSR J1723-2837	538.87	−2.19	0.93	−15.18	−0.67	0.74	1.0
PSR J1740-5340A	273.95	−12.6	2.2	−1.99	−12.40	17.25	2.5
PSR J1748-2021D	74.10	−3.22	8.24	−0.04	−3.22	230.91	0.6
PSR J1816 + 4510	313.17	−4.227	4.36	−2.98	−3.93	6.95	0.7
PSR J1906 + 0055	358.48	−0.427	4.48	−4.47	...	...	...
PSR J1957 + 2516	252.42	−1.748	2.66	−1.56	−1.59	7.59	0.8
PSR J2215 + 5135	383.2	−4.9	2.77	−5.46	−4.35	4.42	1.0
PSR J2339-0533	346.71	−1.695	1.1	−4.04	−1.29	3.09	1.4

These sources can be detected by the third-generation GW detectors like Einstein Telescope. **(Chen 2020, PRD)**

Ultracompact binary pulsars

(Tauris 2018, PRL)

Compact NS+WD
Dual-line GW sources

Orbital shrinkage of binary pulsars

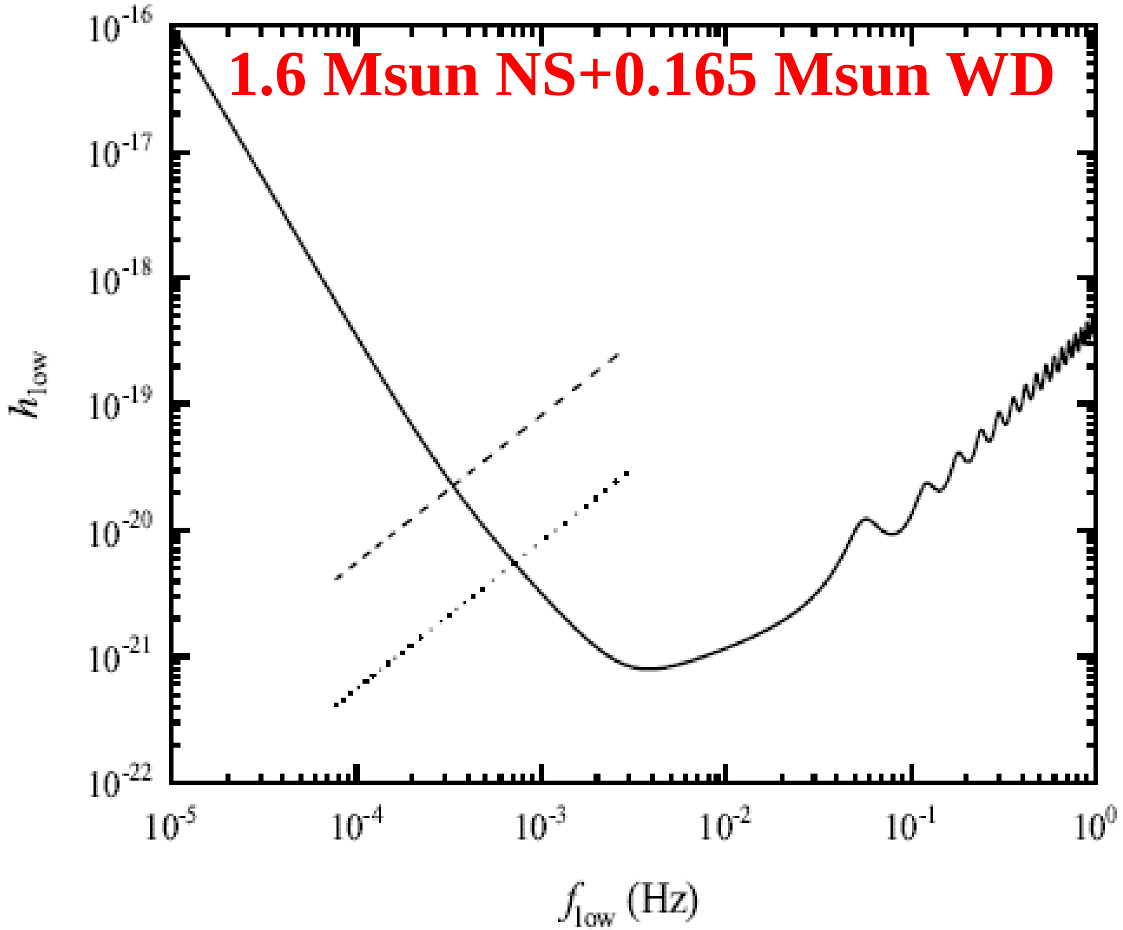

$$h_{low} \approx 3.75 \times 10^{-19} \left(\frac{f_{low}}{1\ \text{mHz}}\right)^{7/6} \left(\frac{\mathcal{M}}{1\ M_\odot}\right)^{5/3} \times \left(\frac{1\ \text{kpc}}{d}\right),$$

a correlation between WD mass and orbital period, $P_{orb,i}$=0.3 days

WD fills its Roche lobe in UCXBs $f_{low,f}$=6.9-7.4 Hz

Chen 2021, PRD

Detection timescales 180 (1 kpc), and 23 Myr (10 kpc)

the timescale of orbital decay is about 8.7 Gyr

Spin-down of NSs with an ellipticity

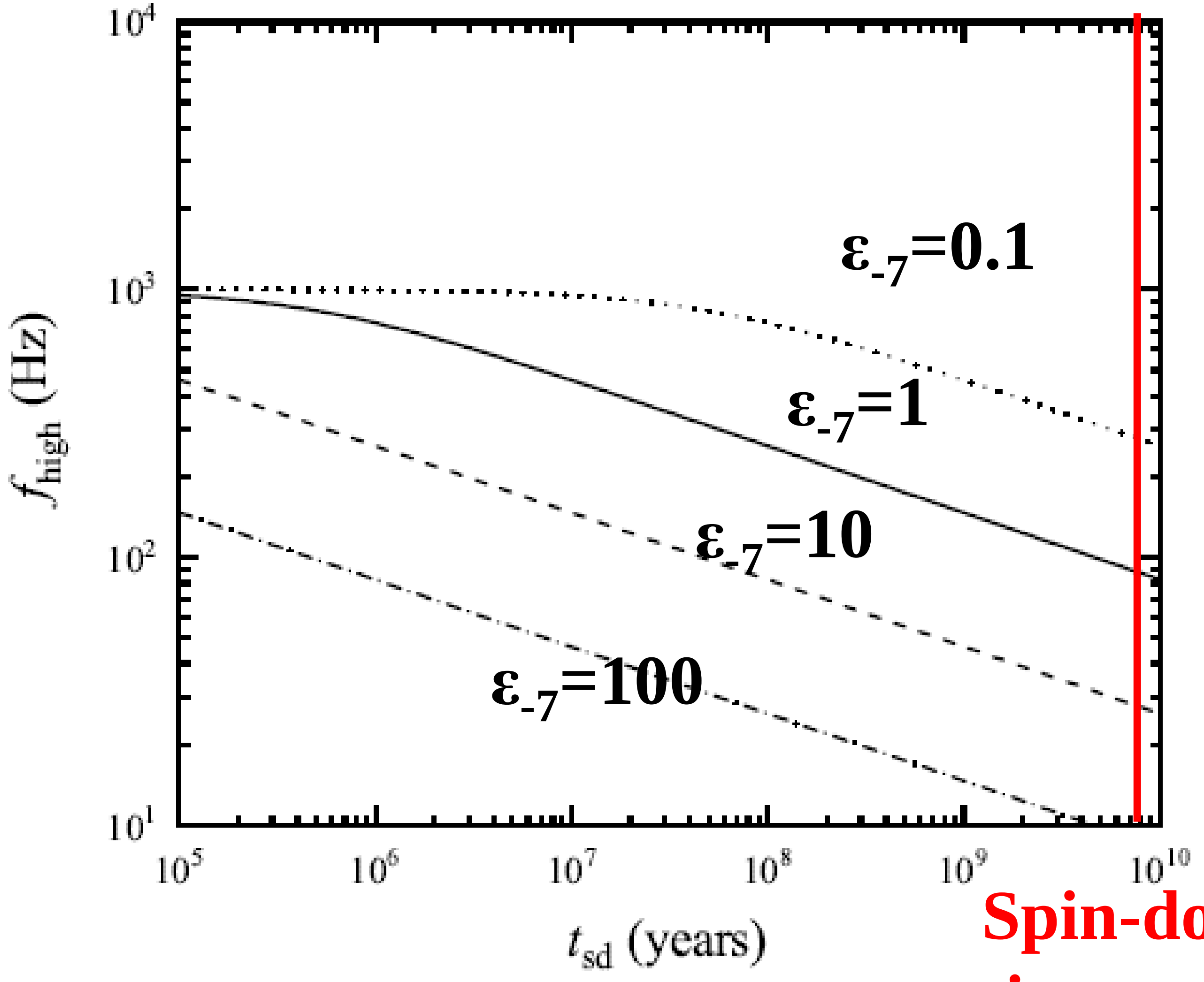

Spin-down timescale 8.7Gyr

- **If the GW radiation is the dominant mechanism influencing the spin evolution of MSP,**

$$f_{high} = \frac{f_{high,0}}{(6.8 \times 10^{-26} \epsilon_{-7}^2 I_{45} f_{high,0}^4 t_{sd} + 1)^{1/4}}.$$

TABLE I: Some input and derived parameters for NSs emitting high-frequency GW signals.

Samples	initial spin period (ms)	$f_{\mathrm{high},0}$ (Hz)	d (kpc)	t_{de} (Gyr)	ϵ_{-7}	f_{high} (Hz)	$\dot{J}_{\mathrm{gr}}$ ($\mathrm{g\,cm^2s^{-2}}$)	$\dot{J}_{\mathrm{md}}$ ($\mathrm{g\,cm^2s^{-2}}$)	τ_{gw} (Gyr)	h_{high}
1	1	2000	10	8.7	1	86	2.5×10^{29}	4.9×10^{27}	33	8.1×10^{-24}
2	2	1000	10	8.7	1	86	2.5×10^{29}	4.9×10^{27}	33	8.1×10^{-24}
3	2	1000	10	6.0	1	94	4.0×10^{29}	6.4×10^{27}	23	1.0×10^{-23}
4	2	1000	10	8.7	10	27	7.7×10^{28}	1.5×10^{26}	34	4.4×10^{-24}
5	2	1000	10	8.7	20	19	5.3×10^{28}	5.3×10^{25}	35	3.7×10^{-24}
6	2	1000	10	8.7	50	12	3.4×10^{28}	1.3×10^{25}	35	3.0×10^{-24}
7	2	1000	10	8.7	0.1	270	7.7×10^{29}	1.5×10^{29}	34	1.4×10^{-23}
8	2	1000	10	8.7	0.01	769	1.5×10^{30}	3.5×10^{30}	51	1.9×10^{-23}

invalid

Chen 2021, PRD

The frequencies of high-frequency GW signals are 10-100 Hz when the ultracompact binary pulsars appear as low-frequency GW sources

Detectability of high-frequency GW signals

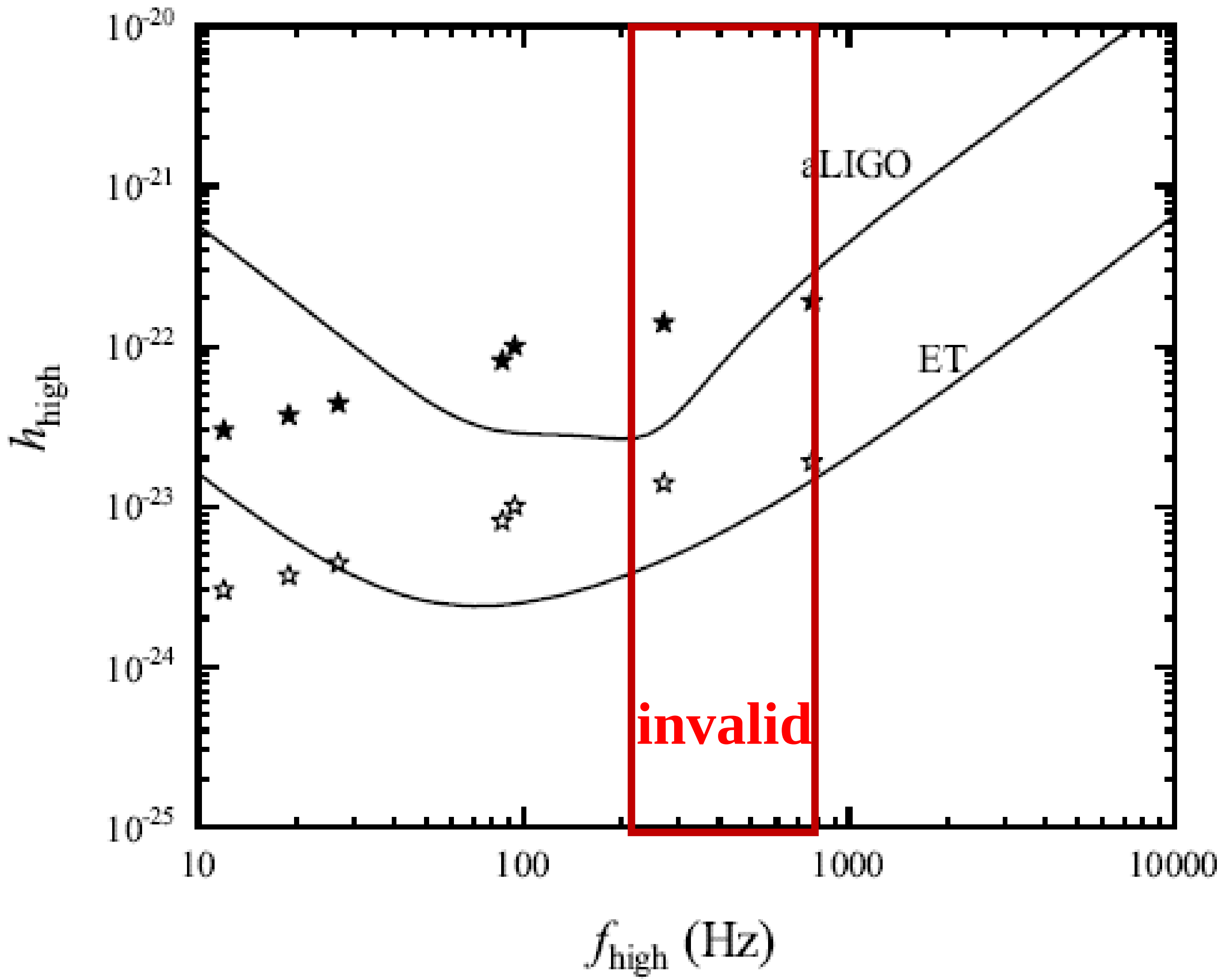

Chen 2021, PRD

high-frequency GW signals with ~100 Hz can be detected by aLIGO within a distance of 1 kpc , while ET can detect a wide frequency range of 10–100 Hz.

For GW signals with a frequency of ~100 Hz, the detection horizon of ET can reach 10 kpc.

Significance of dual-line detections

- **Detections of dual-line GW signals yield**

$$\epsilon I = 1.0\times 10^{44}\left(\frac{10\ \mathrm{Hz}}{f_{\rm high}}\right)^{5/2}\left(\frac{f_{\rm low}}{1\ \mathrm{mHz}}\right)^{7/6}\times\left(\frac{\mathcal{M}}{1\ M_\odot}\right)^{5/3}\left(\frac{h_{\rm high}}{h_{\rm low}}\right)\ \mathrm{g\,cm^2}.$$

- **From the detections of high-frequency GW signals, we can obtain**

$$\epsilon^2 I = -5.8\times 10^{34}\left(\frac{\dot f_{\rm high}}{10^{-17}\ \mathrm{Hz\,s^{-1}}}\right)\left(\frac{10\ \mathrm{Hz}}{f_{\rm high}}\right)^5\ \mathrm{g\,cm^2}$$

I and ϵ are independent of the distance, and depend on five observed parameters $f_{\rm low}$, $f_{\rm high}$, $h_{\rm low}$, $h_{\rm high}$, and *chirp mass*.

NS radius can be calculated from the derived I and Mns, and then the EOS of NSs can be constrained

Conclusions

- **When the ellipticities of NSs are (1–50)× 10^{-7}, compact binary pulsars can become dual-line GW sources**
- **High-frequency GW signals have a frequency of 10-100 Hz, and can be detected by aLIGO or ET.**
- **Dual-line GW sources can help us to constrain EOS of NSs.**
- **Confirmation for dual-line GW sources must depend on the observed parameters of known binary pulsars.**

Thank you!